ELSEVIER

Polymer Vol. 37 No. 2, pp. 253–261, 1996

0032-3861/96/$15.00+0.00

Self-diffusion coefficient distributions in solutions containing hydrophobically modified water-soluble polymers and surfactants

K. Persson*, P. C. Griffiths† and P. Stilbs
Physical Chemistry, Royal Institute of Technology, Stockholm S 100 44, Sweden
(Received 26 September 1994)

The self-diffusion coefficient distribution, obtained from an inverse Laplace transform of the pulsed-gradient spin-echo nuclear magnetic resonance attenuation function, has been studied as a function of both associative polymer and surfactant concentration. Compared to the parent homopolymer, the associative polymer exhibited a much wider distribution of self-diffusion coefficients, which narrows with surfactant concentration. When the surfactant concentration reaches the saturation level for the polymer, the width of the distributions of the parent homopolymer and associative polymer become identical. The structural basis for these observations is discussed.

(Keywords: water-soluble polymers; hydrophobic modification; self-diffusion coefficient)

INTRODUCTION

Hydrophobically modified water-soluble polymers in today's technologies have found widespread applications as viscosity modifiers. The idea behind the inclusion of these materials, often called 'thickeners', is to improve the viscosity characteristics of products, such as for example water-based paints[1]. However, these formulations contain many components with diverse properties and, thus, a fundamental understanding of the interaction of the polymer with these other components is necessary.

Hydrophobically modified polymers self-associate in aqueous solution by virtue of their insoluble moieties. Self-association phenomena have been studied by a wide range of techniques, including viscosity[2–7], static and dynamic fluorescence[8–10], static and dynamic light scattering,[11,12], microcalorimetry[13], e.s.r.[14] and n.m.r. self-diffusion and spin relaxation[3,9,15,16].

At low concentrations, it is generally accepted that these thickeners form micelle-like structures, which gradually interact with increasing concentration[8,10,13,14,17]. These micelle-like structures are here called *primary aggregates*. At higher concentrations, the primary aggregates interconnect to form network-like structures called *clusters*.

A model associative polymer (AP) that consists of a 200 monomer unit poly(ethylene oxide) chain that is end-capped with C_{12} alkyl groups ($C_{12}EO_{200}C_{12}$) has been developed in our laboratory[16]. This model associative polymer has been previously studied by n.m.r. relaxation and self-diffusion measurements[13,16].

* To whom correspondence should be addressed
† Permanent address: Department of Chemistry, University of Wales Cardiff, PO Box 912, Cardiff CF1 3TB, UK

^{2}H spin-relaxation data for the associative polymer–sodium dodecyl sulfate (AP–SDS) system have shown that the SDS motions could be described by a two-step model comprising (i) the anisotropic, localized motion of the SDS molecules in the core of the micelle and (ii) the slower, isotropic motions arising from a combination of lateral diffusion of the SDS molecules over the curved surface of the micelle and the 'tumbling' of the whole aggregate[16]. The local motion of SDS was slower in the mixed aggregate than in pure surfactant micelles, but was found to be largely unaffected by the amount of polymer. The slower process, on the other hand, was substantially retarded in the presence of AP due to the greater size of this aggregate. A parallel ^{2}H spin-relaxation study of the polymer showed that there was a further very slow motional component present in the dynamics of the polymer.

Concomitant with an increase in concentration of the AP, one finds a decrease in the self-diffusion coefficient and an increase in its polydispersity[3,9,13,16]. In the presence of SDS, the self-diffusion coefficient of the AP can either increase or decrease with increasing SDS concentration[9,13] depending on the AP concentration. However, the polydispersity index of the self-diffusion-coefficient is markedly smaller for all SDS concentrations. Dependent on the concentration ratio of polymer to surfactant, and the polymer molecular weight, the structure of the aggregate varies dramatically[9,13].

Several types of motion obviously exist in these systems, each described by a characteristic distance scale and timescale. Discussing the diffusion behaviour in terms of a single self-diffusion coefficient, therefore, seems rather simplistic. One attempt to extend this

analysis is to invoke a stretched exponential analysis where the level of 'stretching' is related to a phenomenological parameter, β, describing the width of the distribution. In the present paper, an inverse Laplace transformation (*ILT*)[18,19] has been applied to attenuation functions to extract the self-diffusion coefficient distribution present in the sample. It is shown how more detailed representations of the self-diffusion coefficient distribution can be informative in the study of these systems.

EXPERIMENTAL

Samples

The model associative polymer, poly(ethylene oxide) didodecyl ether, $C_{12}EO_{200}C_{12}$ ($M_w = 9300$, $M_w/M_n = 1.1$), was synthesized in-house by Ann-Charlotte Helgren[16]. The parent poly(ethylene oxide) (PEO) sample ($M_w = 10\,000$, $M_w/M_n = 1.05$) was purchased from Fluka. The lower molecular weight of the AP might be due to some degradation during synthesis. Surface tension measurements suggest the presence of a very small amount of hydrophobic impurity. The extent of substitution was determined by ^{1}H n.m.r. to be greater than 90%. The following surfactants were used in the n.m.r. measurements: sodium dodecyl sulfate (Fluka), twice recrystallized from ethanol; dodecyltimethylammonium bromide (DTAB), recrystallized from CCl_4; and poly(ethylene oxide) dodecyl ether, $C_{12}E_{23}$ (Sigma), used with no further purification. The n.m.r. samples were prepared by using ^2H_2O (Isotec Inc., 99.9%) and were tumbled for 1 h and allowed to equilibrate at room temperature for 24 h prior to measurements.

N.m.r. self-diffusion measurements

The self-diffusion measurements, using the Fourier-transform pulsed-gradient spin-echo (PGSE) n.m.r. technique[20], were performed on a Bruker MSL200 spectrometer employing the longitudinal eddy current delay (LED) sequence[21]. The attenuation of the spin-echo amplitude after Fourier transformation was sampled as a function of the duration, δ, of the applied gradient pulse ($0.2 \leq \delta \leq 6.5$ ms). The r.f. pulse interval, τ, was fixed at 10 ms during the experiments in order to keep spin–spin relaxation time, T_2, effects on the echo amplitude to a minimum. The gradient pulse interval, Δ, was kept constant at 400 ms while its magnitude, G, was also varied between 0.17 and 2.2 T m^{-1}. Field gradient calibration was carried out by the use of known self-diffusion standards ($H_2O/^2H_2O$ mixtures)[22]. A constant temperature of 25°C was used.

For molecules undergoing unhindered Brownian motion, the decay of the echo amplitude $A(\delta)$ obeys:

$$A(\delta) = A(0)\exp(-kD_s) \qquad (1)$$

Here $k = (\gamma G\delta)^2(\Delta - \delta/3)$ where γ is the magnetogyric ratio of the nucleus under observation (in this case, protons) and D_s represents the self-diffusion coefficient. The self-diffusion coefficient of the AP was derived from the attenuation of the ethylene oxide peak occurring at 3.75 ppm, although the peaks from the alkyl end-groups yield the same result.

THE INVERSE LAPLACE TRANSFORMATION AS APPLIED TO PGSE N.M.R. ATTENUATION FUNCTIONS

With the exception of those solutions containing surfactant at a sufficient concentration to saturate the polymer, the attenuation functions show varying degrees of upward concavity, indicating the presence of a finite distribution of self-diffusion coefficients. The purpose of this paper is to examine whether the distribution correlates with the surfactant type and concentration.

Provencher's CONTIN[18,19] approach has previously been applied to PGSE n.m.r. data by Johnson *et al.* and the problems associated with this particular application have been discussed in considerable detail[23–25]. We will only summarize the salient features in the following discussion.

An inverse Laplace transformation (*ILT*) applied to an attenuation function offers a valuable opportunity to extract the self-diffusion coefficient distribution present in the sample. This information, in principle, contains the size distribution of the diffusing species and provides an insight into complex dynamic systems that can be gained from no other experiment. Although this type of inversion is ill-posed and often intractable, there is a computer algorithm, CONTIN, widely distributed for this purpose[18,19].

Consider, from a theoretical standpoint, the diffusion experiment as given by equation (1). It is clear that a single self-diffusion coefficient will yield an exponential function. The *ILT* is effectively determining what range of time constants will fit this data within some statistical boundary. Given the fact that there is no noise in this infinite-time, theoretical data set, the *ILT* would return a delta function with infinitesimal width located at a position on the x-axis corresponding to the time constant of the decay—the self-diffusion coefficient. By analogy with equation (1), it may be seen that the height of this delta function corresponds to the intensity of the n.m.r. signal when $G = 0$, i.e. $A(0)$.

By contrast, a theoretical, noise-less biexponential function would, upon *ILT*, yield two delta functions located on the x-axis at positions corresponding to the two time constants. These two functions would also have infinitesimal width given sufficient resolution over the necessary time windows. A theoretical, noise-less attenuation function arising from a smooth distribution of time constants when subjected to an *ILT*, however, would yield a number of possible solutions and, hence, the resultant distribution would have a finite width.

With these factors in mind, consider now a 'real', noisy attenuation function arising from the measurement of a monodisperse system with only a single self-diffusion coefficient. By virtue of the noise, a set of diffusion coefficients will fit the data to a comparable statistical quality, and the resultant distribution is inherently broadened. In this situation the set of self-diffusion coefficients selected as possible solutions may be substantially reduced by using optimum experimental parameters—a signal which decays into noise and is sampled with a large number of points. Even with these criteria, a distribution of self-diffusion coefficients is obtained and the intensity of each self-diffusion coefficient provides the signal intensity for equation (1). The situation is further exasperated when the system is not

monodisperse and a range of self-diffusion coefficients exists. The set of self-diffusion coefficients selected as possible solutions is inherently non-unique but is then sensitive to how the time function has been sampled, i.e. the number and separation of the data points, as well as the time window itself. The result of this is that the intensity of each contributing self-diffusion coefficient to the overall attenuation function is, thus, somewhat dependent on the experimental parameters.

DATA TREATMENT

The *ILT* is nonetheless a valuable procedure and useful data can be obtained, although care must be taken to minimize any artefacts that may be introduced through 'inconsistent' data treatment. Thus, a set of guidelines have been followed to minimize such problems:

(i) The intensities of the individual self-diffusion coefficients in the distribution depend on the signal intensity of the particular experiment. This random dependence can be largely removed by normalizing the signal intensity to the first point in the decay, where k is effectively zero. In this way, all the experiments decay from unity.

(ii) For greater curvature in the attenuation plot, the inversion procedure requires a wider range of self-diffusion coefficients to sample the decay adequately. This has the effect of increasing the point spacing (decreasing resolution) in the self-diffusion coefficient distribution. When the curvature is minimal, the same input parameters lead to a much narrower distribution, with all the signal intensity occurring in a few closely spaced bands. Inherently, the intensity of this latter distribution is considerably greater. Simply as an aid to visualizing the observed trends, the distributions have been normalized so that the area under each distribution is equivalent on a linear scale. This normalization has been achieved by dividing each point of the distribution by the total area under the curve.

RESULTS AND DISCUSSION

A typical attenuation function is shown in *Figure 1* in the form of equation (1). As may be seen, there is a significant curvature in the data, signifying the presence of a distribution of diffusion coefficients. Attempting to fit the data to equation (1) (chain line) is unsuccessful. Also shown are the CONTIN (solid line) and stretched exponential analyses[13] (dotted line). Over the entire time window (main diagram) there is little to separate these two representations. This fact is reflected in the agreement between the position of the maximum in the distribution and mean self-diffusion coefficient obtained from the stretched exponential analysis—an agreement that was found for all the systems investigated. Shown in the inset is the initial portion of the same attenuation function and both the CONTIN and stretched exponential fits. The CONTIN fit gives a slightly better representation of the data, but both fits are within the accuracy of the experiment.

In the following sections, raw data of a previously published study[13] have been re-evaluated using the inversion procedure and will be compared with the conclusions drawn from that study. To assist the reader, the behaviour of the self-diffusion coefficient as perceived by the stretched analysis will be discussed first, followed by the additional information gained from the CONTIN inversion analysis.

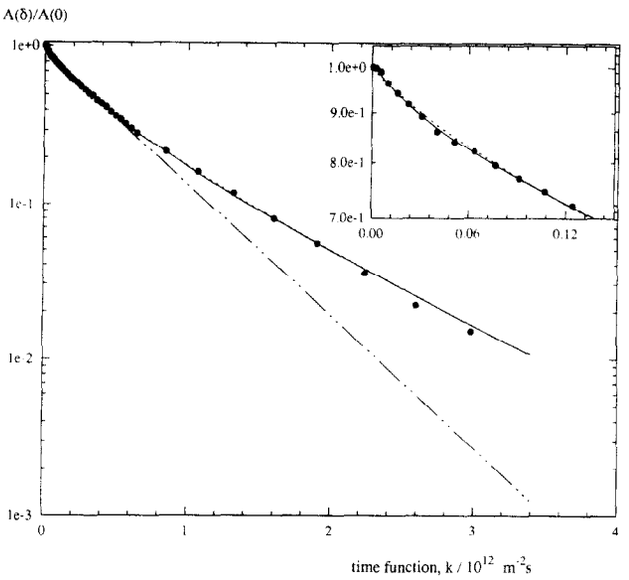

Figure 1 A typical experimental attenuation function for the EO peak of the AP in aqueous solution. Also shown are the single component fit (chain line), the stretched exponential fit (dotted line) and the CONTIN fit (solid line)

Self-association of $C_{12}EO_{200}C_{12}$

Recapitulation of the results of single and stretched exponential analyses[13]. At low concentrations, the self-diffusion coefficient of both the AP and the parent PEO are of the same order of magnitude. Indeed at infinite dilution, they converge to a common point. Self-association starts at a critical aggregation concentration (*CAC*) of 0.013 wt %[13,26]. At low concentrations, although above *CAC*, the average separation of the primary aggregates is such that little bridging by the AP chains might be expected. With increasing AP concentration, there is an increase in the number of AP aggregates and a concomitant reduction in the AP aggregate separation. Once the separation has exceeded some critical value, the primary aggregates interact much more strongly. Consequently, with increasing polymer concentration, the AP self-diffusion coefficient decreases much more rapidly than the self-diffusion coefficient of the parent PEO. By 10 wt % polymer content, the self-diffusion coefficient of the AP is some two orders of magnitude smaller than that of the parent PEO. Whilst the PEO could be described by a single self-diffusion coefficient, the AP showed a significant polydispersity, which increased with increasing AP concentration. For example, fitting the stretched exponential analysis of a 0.5 wt% AP solution yields $\beta = 0.85$. For $\beta < 0.85$, the ratio $D_{mean}/D_{app} < 0.9$ and care must be taken to ensure that this type of analysis adequately describes the distribution of self-diffusion coefficients. For the purposes of this paper, the 0.5 wt % sample will be discussed as an illustration. It should be remembered, however, that this discussion is equally pertinent to all AP concentrations.

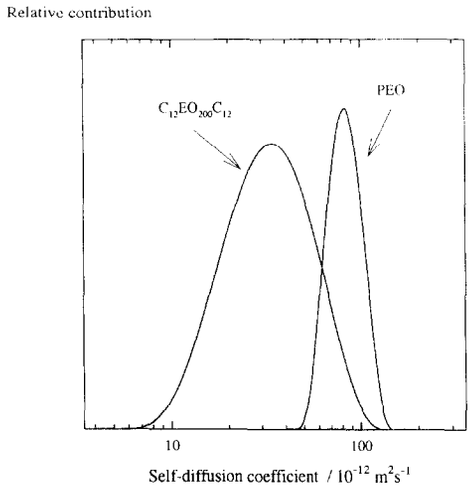

Figure 2 A representation of the CONTIN analysis of the self-diffusion coefficient distribution of 0.5 wt % $C_{12}EO_{200}C_{12}$ and 0.5 wt % PEO

CONTIN analysis. Consider the CONTIN analysis of the 0.5 wt % system shown in *Figure 2*. Both the AP and the parent PEO are displayed. As may be seen the parent PEO exhibits a distribution with a width comparable to the natural broadening inherent in the analysis[27]. Given the monodisperse nature of the polymer, this distribution is reasonable. The position of the distribution is in excellent agreement with the single and mean self-diffusion coefficients obtained from the previous analyses[13]. By contrast, however, not only is the width of the self-diffusion coefficient distribution for the AP substantially greater than for the parent PEO, but the position of the distribution maximum is also considerably lower. Both effects originate from the self-association of the AP. As found throughout this work, the maximum agrees well with the mean self-diffusion coefficient obtained from the stretched exponential analysis[13]. From the width of the self-diffusion coefficient distribution, it is clear that there must be a considerable polydispersity in the size of the diffusing species. This width can only be explained assuming that a small, but significant, proportion of the PEO chains bridge between primary aggregates. Whilst the average separation of the primary aggregates suggests that this is improbable, those aggregates bridged by such chains would attain a lower than average separation. (The average separation is 350 Å compared to the root mean square end to end distance including the end groups, R_{AP}, of one AP which is 142 Å, as discussed further in the 'summary' later in this section.)

Polymer–SDS interactions at low AP concentration

The surfactant SDS interacts with the AP in solution in two different manners: first, through the polymer end-groups and, subsequently, through the EO backbone. The first type of interaction takes place at very low SDS concentrations—for an AP concentration of 0.05–0.1 wt %, the end-groups are saturated above 2 mmol kg^{-1} and association of SDS with the EO chain starts[13]. This association is only present above a solution concentration of 4 mmol kg^{-1} SDS for the parent PEO[13,28,29].

Recapitulation of the result of the single and stretched exponential analyses[13]. With increasing SDS concentration, the self-diffusion coefficient of the AP increases rapidly up to a maximum value that depends on the polymer to surfactant concentration ratio. The increasing self-diffusion coefficient was interpreted as being representative of the break-up of the polymer aggregates by the interaction with SDS. After the maximum in the self-diffusion coefficient vs. SDS concentration behaviour, the self-diffusion coefficient behaviour of the AP is analogous to the PEO–SDS complex. The effects of the end-groups have thus vanished as they became saturated with SDS. The stretched exponential analysis also showed that the self-diffusion coefficient behaviour approaches that of a monodisperse polymer solution in that β approaches unity. PEO of a similar molecular weight, when saturated with SDS, interacts with only one SDS micelle[30–32]. It is most likely, therefore, that when saturated with SDS, a high proportion of the AP molecules will have both their end-groups associated with the same SDS micelle–a point that will also be further discussed.

CONTIN analysis. The CONTIN analysis for this system is shown in *Figure 3*. The most marked difference between the no-surfactant and the surfactant-saturated cases is the much narrower width of the AP self-diffusion coefficient distribution in the latter case. Whilst this could be inferred from the β values, the distribution itself was not known. The β analysis is also dependent on the shape of the self-diffusion coefficient distribution.

Comparing the AP and PEO self-diffusion distributions given in *Figure 3*, it may be seen that the effects of the end-groups have been removed in 180 mM SDS solutions—as the two distributions are essentially the same. The agreement between the position of the AP and PEO distributions confirms that the sizes of the aggregates are no longer influenced by hydrophobic interactions between the AP end-groups.

The physical significance of this substantial narrowing of the AP self-diffusion coefficient distribution is that the heterogeneity of the clusters (of primary aggregates) must be greatly reduced, i.e. the cluster size distribution is far more monodisperse. The small fraction of PEO

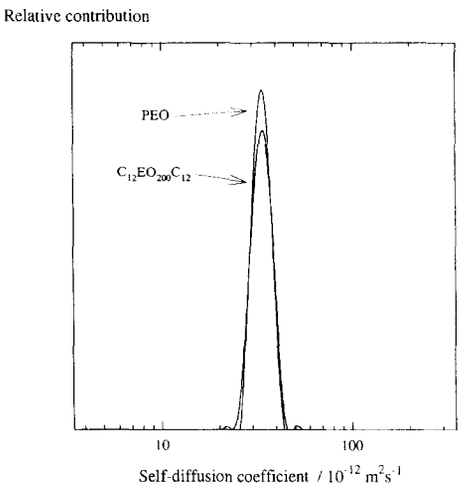

Figure 3 A representation of the CONTIN analysis of the self-diffusion coefficient distribution of 0.5 wt % $C_{12}EO_{200}C_{12}$ and 0.5 wt % PEO in solution with an SDS concentration of 180 mM

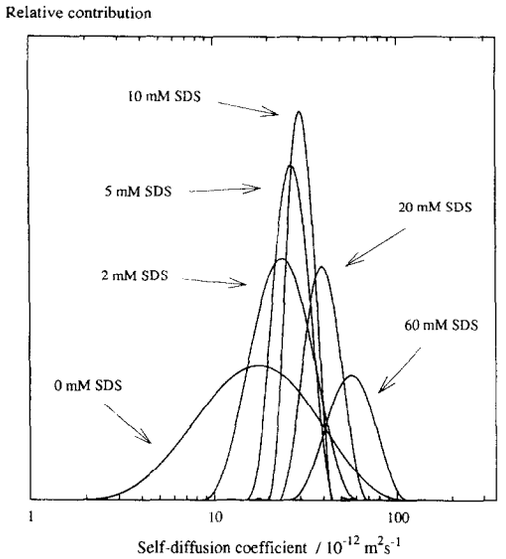

Figure 4 A representation of the CONTIN analysis of the self-diffusion coefficient distribution of 1.0 wt % $C_{12}EO_{200}C_{12}$ as a function of SDS concentration. SDS concentration shown inset

chains acting as bridges between primary aggregates at low AP concentrations have now been able to rearrange so that an even greater proportion of AP molecules have both end-groups in the same hydrophobic core. The size of this *mixed micelle* is then comparable to the size of the PEO–SDS aggregate, and since little bridging is present, the self-diffusion coefficient distributions become similar. The driving force behind this rearrangement is discussed in the 'summary' later in this section.

A visual representation of the narrowing process is shown by the self-diffusion coefficient distributions given in *Figure 4* for a 1 wt % AP solution as a function of SDS concentration. With increasing SDS concentration, the distribution narrows as the effects of the end-group association are removed. There is a concomitant movement of the self-diffusion coefficient distribution to higher values as the network is gradually dispersed. The positions of the distributions are in excellent agreement with the values of the self-diffusion coefficients obtained from the stretched exponential analysis.

Polymer–SDS interactions at higher AP concentration

Recapitulation of the results of the single and stretched exponential analyses[13]. The self-diffusion coefficient of the AP in more concentrated solutions responds differently to the addition of surfactant. In 2.5 and 5 wt % solutions, the stretched exponential analysis shows that the AP self-diffusion coefficient initially decreases and displays clear minima at about 20 and 40 mmol kg^{-1} SDS respectively, before increasing at higher surfactant concentrations.

CONTIN analysis. The self-diffusion coefficient distribution for the 2.5 wt % sample are displayed in *Figure 5* as a function of SDS concentration. *Figure 5a* shows the region where the stretched exponential analysis indicated that the self-diffusion coefficient decreases with increasing concentration of SDS, whilst *Figure 5b* contains the region where the stretched exponential analysis suggested the opposite behaviour–an increase in the

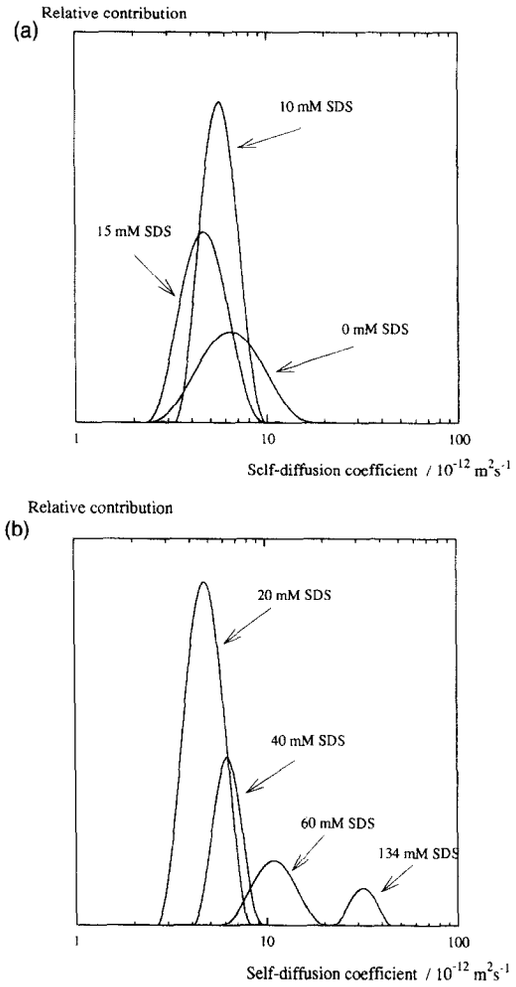

Figure 5 Representations of the CONTIN analysis of the self-diffusion coefficient distribution of 2.5 wt % $C_{12}EO_{200}C_{12}$ as a function of SDS concentration. SDS concentration shown inset

self-diffusion coefficient with increasing SDS concentration. The distributions obtained from the *ILT* for these systems follow exactly the same trend as the stretched exponential analysis. In the two highest SDS concentrations the position of the self-diffusion coefficient distribution is invariant—reflected also in the plateau of the stretched exponential self-diffusion coefficient vs. SDS concentration behaviour[13].

Notice the behaviour of the width of the distribution. With increasing SDS concentration, the width of the distribution decreases monotonically from its maximum value for the no-surfactant case to the surfactant-saturated level. Addition of surfactant causes a reinforcement of the network as shown by the decrease in both the stretched exponential estimate of the self-diffusion coefficient and the position of the self-diffusion coefficient distribution. The decrease in the widths suggests that some 'homogenizing' of the aggregate structure is occurring—end-groups from the same AP molecule are able to bridge between adjacent aggregates, resulting in more bridged aggregates and a decrease in the mobility. With further increases in SDS concentration, the aggregates become saturated with SDS and eventually the network is disrupted.

The corresponding behaviour of the 5 wt % AP system is shown in *Figure 6*. Although the changes in the width of the distribution are less obvious at this

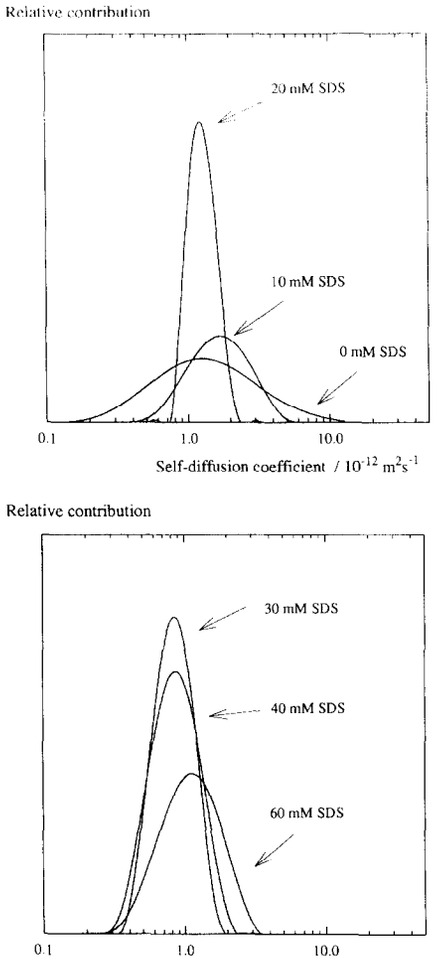

Figure 6 Representations of the CONTIN analysis of the self-diffusion coefficient distribution of 5 wt % $C_{12}EO_{200}C_{12}$ as a function of SDS concentration. SDS concentration shown inset

concentration compared to the 2.5 wt % case, the same general trends exist. For an equivalent concentration ratio of SDS to AP, the 2.5 and 5 wt % systems behave similarly, except for the absolute magnitude of the self-diffusion coefficient.

Summary of SDS–AP interactions

Any summary of the association behaviour of SDS and the AP must be concerned with the relative magnitudes of the interactions due to the hydrophobic nature of the end-groups and the enthalpic interactions between the segments comprising the PEO backbone and the solvent. Water is a good solvent for PEO and, therefore, the PEO chain is expected to adopt a configuration in solution to maximize its solvent–segment contacts.

At low AP concentrations, the separation of the end-groups of adjacent primary aggregates is such that any bridging that occurs would be unfavourable due to the high level of stretching the PEO chain must adopt. Indeed, simple model calculations using the average aggregation number determined by fluorescence quenching, ~ 31 end groups[14,26], suggest that the average centre–centre separation of the primary aggregates is 350 Å at a concentration of 0.5 wt % whereas the radius of gyration, R_g, of the AP is 142 Å. Some chains may, even so, have their end-groups in different primary aggregates in order to decrease the steric constraints around the primary aggregate and thus facilitate the required aggregation number. Annable *et al.* describe these conformations of the AP molecules as *loops* and *bridges*[33,34]. Both of these configurations are entropically unfavourable, but such is the strength of the hydrophobic effect. The cluster-promoting *bridging* will have the effect of reducing the self-diffusion coefficient compared to primary aggregates that have no bridged AP molecules. The reduction in the self-diffusion coefficient accordingly depends on the level of bridging. This bridging effect also reduces the diffusion coefficient compared to the parent PEO, which could be regarded as discrete polymer chains in solution. The heterogeneity in the size of the diffusing species caused by the presence of the small, but significant, fraction of bridged AP chains results in the wide self-diffusion coefficient distribution.

At higher AP concentrations, the number of aggregates increases and their separation decreases. At a concentration of 2.5 wt %, the centre–centre separation of the primary aggregates is 205 Å, assuming that the aggregation number is independent of concentration. This separation is now only slightly greater than the R_{AP} of the AP (142 Å). The entropically unfavourable conformations arising from chain stretching or collapse are now relaxed somewhat since the primary aggregates are more accessible to all end-groups. Thus, the AP molecules can adopt a conformation much more akin to the solution configuration of the parent PEO. The increase in the number of hydrophobic interactions involving bridged AP molecules results in a stronger network and, hence, smaller self-diffusion coefficient. With increasing concentration of AP, therefore, the structure develops from one consisting of predominately looped AP molecules forming few bridged hydrophobic aggregates to a structure comprising many more bridges—the balance between loops and bridges has moved more towards bridges since the primary aggregates are closer together. At the highest AP concentration studied, 5 wt %, the average separation of the primary aggregates is 163 Å and smaller than the R_{AP} of the AP. Thus, it seems more likely that the end-groups of each particular AP molecule reside in different primary aggregates, i.e. predominantly in the form of bridges with few loops.

This loop vs. bridge picture offers an insight into the different response of low- and high-AP-concentration systems to the addition of surfactant. At low AP concentrations, the strong hydrophobic effect dominates and results in the AP chains adopting unfavourable conformations. The initial addition of SDS, preferentially solubilized in the AP end-group region, will result in a decrease in the relative magnitude of the hydrophobic interaction between the end-groups. In other words, the SDS aggregated AP end-groups will be slightly less hydrophobic since the polar SDS head-groups are able, partially at least, to solubilize them. Under these circumstances, the entropically unfavourable polymer conformation may dominate this balance and the conformation can be relaxed—the highly stretched, bridged chains are able to explore the local solution, searching for closer primary aggregates, or indeed, existing simply as SDS solubilized end-groups. Similarly, compressed loops will be able to search for more distant primary aggregates, although to a much lesser degree given the average

separation of the primary aggregates. This will result in an increase in the self-diffusion coefficient, since the level of bridging is reduced, and a narrowing of the self-diffusion coefficient distribution, because the extremes of stretched/compressed chains will be 'released' first. The process continues with further addition of SDS until both the backbone and all end-groups are saturated. At this point, the AP–SDS aggregate resembles the parent PEO–SDS aggregate, with the AP end-groups located in the core of the micelle–as reflected by the self-diffusion coefficient behaviour.

At higher AP concentrations, the SDS aggregates with the end-groups as in the low-AP-concentration systems. However, for intermediate AP concentrations, since the distribution of the looped and bridged chains is different, the AP end-groups are not forced through entropic arguments to reorganize significantly and, thus, can remain in the mixed micelle. Initial additions of SDS, therefore, merely move the loop vs. bridge balance slightly in favour of the bridged AP molecules, i.e. the primary aggregates become more uniformly bridged. This results in a narrower self-diffusion coefficient distribution at slightly lower absolute values. At higher SDS concentrations, once the end-groups have been saturated, the network will become disrupted. With increasing AP content the sensitivity of the position of the self-diffusion coefficient distribution as a function of increasing surfactant concentration decreases, as also found by Annable *et al.*[34].

Once the AP end-groups are saturated with SDS, the SDS will aggregate on the EO backbone. Self-diffusion studies of the SDS on the same solutions have shown that, above a critical ratio of 15 mM for every weight percentage polymer concentration, the concentration of free surfactant in solution is constant. This corresponds to the saturation point of the end-groups, and above this surfactant concentration, the SDS associates with the EO backbone. The association of surfactants onto polymers is believed[30–32,35–39] to occur in a number of discrete locations randomly distributed throughout the solution—initial additions of SDS nucleate micelle growth along the EO backbone whilst subsequent additions will either nucleate further micelles or promote the growth of the existing micelles, depending on the precise nature of the AP system. This results in a random distribution of partly formed polydisperse AP–SDS mixed micelles throughout the system which may account for the slight broadening that is observed in the self-diffusion coefficient distribution above the critical SDS concentration. Whilst this is one explanation, there may be others.

Polymer–DTAB and polymer–$C_{12}E_{23}$ interactions

It is well-known that SDS and PEO interact strongly through the EO backbone[28–32,35–40], whereas DTAB[13,41] and $C_{12}E_{23}$ do not interact with EO to any great extent—the interaction between these surfactants and the AP will be, therefore, through the hydrophobic end-groups only.

The data in *Figure 7* compare the change in the self-diffusion coefficient distribution of a 1 wt % AP polymer solution upon addition of a different type of surfactant, the cationic DTAB. The self-diffusion coefficient distribution obtained from the stretched exponential analysis[13] shows a slight decrease with increasing surfactant concentration–the AP–DTAB interaction appearing to strengthen the network.

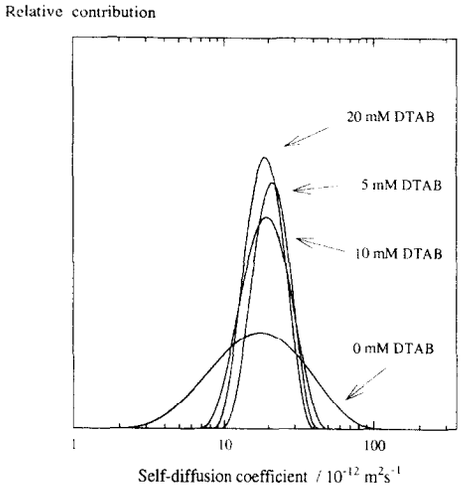

Figure 7 A representation of the CONTIN analysis of the self-diffusion coefficient distribution of 1.0 wt % $C_{12}EO_{200}C_{12}$ as a function of DTAB concentration. DTAB concentration shown inset

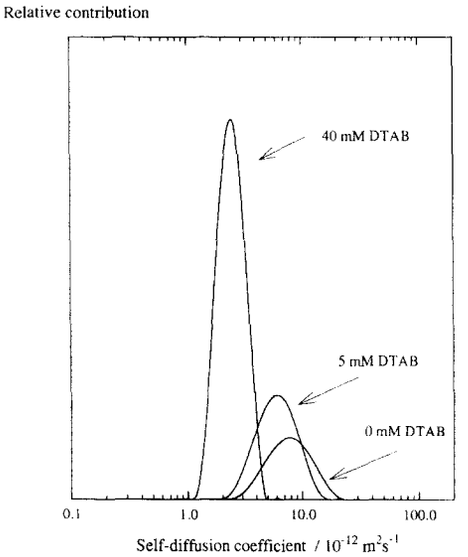

Figure 8 A representation of the CONTIN analysis of the self-diffusion coefficient distribution of 2.5 wt % $C_{12}EO_{200}C_{12}$ as a function of DTAB concentration. DTAB concentration shown inset

With DTAB, the CONTIN analysis suggests a narrowing of the distribution as the DTAB induces some local rearrangement of the small fraction of bridged chains. This results in a homogenizing of the loop vs. bridge balance where larger clusters are broken down into smaller ones and some clustering of non-bridged primary aggregates is induced.

At higher AP and surfactant concentrations, such as that displayed in *Figure 8*, a change in the network has occurred, entailing a decrease in perceived polydispersity of the system and the shift of the self-diffusion coefficient distribution to smaller self-diffusion coefficients.

In the SDS–AP complex, there is a strong affinity for the backbone to be attached to the aggregate surface. However, since DTAB does not exhibit this interaction, the PEO chain extends into solution rather like a large 'loop'. By comparison with the 40 mM SDS case given in *Figure 5b*, it may be seen that the DTAB–AP complex has a smaller self-diffusion coefficient and is therefore larger in size, as expected.

In this section describing the SDS behaviour, it was

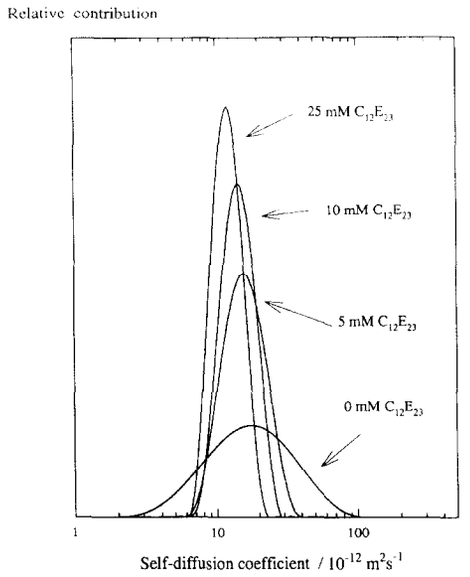

Figure 9 A representation of the CONTIN analysis of the self-diffusion coefficient distribution of 1.0 wt % $C_{12}EO_{200}C_{12}$ as a function of $C_{12}E_{23}$ concentration. $C_{12}E_{23}$ concentration shown inset

proposed that saturating the AP end-group zones with SDS results in a dispersal of the network induced by SDS micelles leaving the hydrophobic zone taking with them a number of AP end-groups. This will only occur if the EO backbone can interact favourably with the surfactant micelle. Since this interaction is absent in the DTAB case, the DTAB solubilized end-groups merely 'hop' between adjacent end-group zones until an optimum balance of the loops vs. bridges is obtained. With increasing surfactant concentration, this balance tends towards bridges, which results in a stronger, less mobile network, i.e. the self-diffusion coefficient decreases. At higher surfactant concentrations, there is evidence to suggest that the network ultimately becomes disrupted[42,42].

Figure 9 displays the self-diffusion coefficient distributions for the AP and the non-ionic surfactant $C_{12}E_{23}$. As in the preceding discussion, there is a considerable difference between the changes induced in diffusion behaviour by this surfactant compared to SDS but little difference compared to the changes induced by DTAB. There is however, a slight decrease in the self-diffusion coefficient with increasing surfactant concentration, probably for the same 'loop vs. bridge balance' reasons given before.

More interesting, perhaps, is this narrowing of the distribution, considering that the distribution must include contributions from both the surfactant and the polymer. Owing to the structural similarity of $C_{12}E_{23}$ and $C_{12}EO_{200}C_{12}$, a unique resonance does not exist with which to separate the two components. The self-diffusion coefficients obtained from the attenuation function of three peaks, $-CH_3$, $-CH_2-$ and $-CH_2-CH_2-O-$, were evaluated for three concentrations of surfactant. In all cases the EO peak gave a slightly wider distribution centred at the same self-diffusion coefficient value. The obvious conclusion that the polymer and surfactant diffuse with similar diffusion coefficients may arise for two reasons: (i) either they diffuse together as a single entity or (ii) the two components have the same self-diffusion coefficient through simple obstruction effects. The latter is less probable since, using the simplest model of obstruction and assuming spherical aggregates, the occupied volume that is needed to account for the observed lowering of the surfactant micelle self-diffusion coefficient would be 40 vol. %. Furthermore results from e.s.r. experiments on the same system[14] clearly show that pure surfactant micelles are not present at these surfactant concentrations. Thus, in solutions where there are more than two AP molecules to every fully grown $C_{12}E_{23}$ micelle, the polymer and surfactant are associated with each other in mixed aggregates.

CONCLUSIONS

The self-diffusion coefficient distributions of a model hydrophobically modified polymer in aqueous solution containing surfactants have been investigated as functions of polymer and surfactant concentration and surfactant type.

There is a substantial polydispersity in the polymer self-diffusion coefficient in aqueous solutions of the AP. The presence of each of the three surfactants studied in this paper significantly narrows this distribution, through effects discussed in terms of a decrease in the number of unfavourable conformations of the polymer. The anionic surfactant SDS was found to have a far larger effect on the position of the distribution than the other investigated surfactants, DTAB and $C_{12}E_{23}$. At sufficiently high SDS concentrations, both the width and the position of the associative polymer self-diffusion coefficient distribution are the same as those for the parent homopolymer. Thus, the effects of the hydrophobically modified end-groups have been nullified.

In the case of the non-ionic micelle, $C_{12}E_{23}$, mixed surfactant–polymer aggregates were favoured over pure surfactant ones, at least when there are more than two AP molecules to each $C_{12}E_{23}$ micelle.

The insight gained through CONTIN has permitted the discussion to be focused more on the structural basis of this heterogeneity. Both the CONTIN and stretched exponential analyses were found to fit the data equally well but, in particular, the width of the distribution obtained from CONTIN is more accessible compared to the phenomenological β parameter. There was, however, a correlation between these two parameters. The position of the distribution was found to be in excellent agreement with the mean self-diffusion coefficient obtained from the stretched exponential analysis.

The stretched exponential analysis is, however, considerably more straightforward and suffers from fewer of the artefacts inherent in an *ILT*. The authors, therefore, suggest that these two analyses be used in conjunction.

REFERENCES

1 Schaller, E. D. and Sperry, P. R. in 'Handbook of Coatings and Additives' (Ed. L. J. Calbo), Vol. 2, Dekker, New York, 1992, pp. 105–163
2 Huldén, M. *Colloids Surf. (A)* 1994, **82**, 263
3 Walderhaug, H., Hansen, F.K., Abrahmsén S., Persson, K. and Stilbs, P. *J. Phys. Chem.* 993 **97**, 8336
4 Fonnum, G., Bakke, J. and Hansen, F. K. *Colloid Polym Sci.* 1993, **271**, 380
5 Huldén M. 'Water-soluble polymers and surfactants in latex paints: competitive adsorption and rheological properties', Ph.D. Thesis, Åbo Akademi University, Finland, 1994

6 Jenkins, R. D. Ph.D. Thesis, Lehigh University, Bethlehem, MD, 1990
7 Lundberg, D. J. Ph.D. Thesis, North Dakota State University, 1990
8 Yekta, A., Duhamel, J., Brochard, P., Adiwidjaja, H. and Winnik, M. A. *Macromolecules* 1993, **26**, 1829
9 Lindblad, C., Almgren, M., Persson, K., Abrahmsén-Alami, S. and Stilbs, P. *Langmuir* submitted
10 Yekta, A., Duhamel, J., Adiwidjaja, H. and Winnik, M.A. *Macromolecules* 1995, **28**, 956
11 Nystrom, B., Walderhaug, H. and Hansen, F. K. *J. Phys. Chem.* 1993, **97**, 7743
12 Seery, T. P., Yassini, M., Hogen-Esch, T. and Amis, E. *Macromolecules* 1992, **25**, 4784
13 Persson, K., Wang, G. and Olofsson, G. *J. Chem Soc, Faraday Trans (1)* 1994, **23**, 3555
14 Persson, K. and Bales, B. L. *J. Chem. Soc., Faraday Trans.* 1995, **17**, 2863
15 Persson, K., Abrahmsen, S. Stilbs, P., Hansen, F. K. and Walderhaug, H. *Colloid Polym. Sci.* 1992, **270**, 465
16 Abrahmsén-Alami, S. and Stilbs, P. *J. Phys. Chem.* 1994, **98**, 6359
17 Baihua, R., Vemura, Y., Dyke, L. and Macdonald, P. M. *Macromolecules* 1995, **28**, 531
18 Provencher, S. W. *Comput. Phys. Commun.* 1982, **27**, 213
19 Provencher, S. W. *Comput. Phys. Commun.* 1982, **27**, 229
20 Stilbs, P. *Prog. Nucl. Magn. Reson. Spectrosc.* 1987, **19**, 1
21 Gibbs, S. J. and Johnson, C. S., Jr *J. Magn. Reson.* 1991, **93**, 391
22 Callaghan, P. T., Le Gros, M. A. and Pinder, D. N. *J. Chem. Phys.* 1983, **79**, 6372
23 Morris, K. F. and Johnson, C. S., Jr *J. Am. Chem. Soc.* 1993, **115**, 4291
24 Morris, K. F. Thesis, University of North Carolina, Chapel Hill, NC, 1993
25 Johnson, C. S., Jr in 'NMR Probes of Molecular Dynamics' (Ed. R. Tycko), Kluwer, Dordrecht, 1994
26 Linblad, C. and Almgren, M., unpublished results
27 Griffiths, P. C. and Stilbs, P. *Langmuir* 1995, **11**, 898
28 Cabane, B. *J. Phys. Chem.* 1977, **81**, 1639
29 Cabane, B. *Colloids Surf.* 1985, **13**, 19
30 Tondre, C. *J. Phys. Chem.* 1985, **89**, 5101
31 François, J., Dayantis, J. and Sabbadin, J. *Eur. Polym J.* 1985, **21**, 165
32 van Stram, J., Almgren, M. and Linblad, C. *Prog. Colloid Polym. Sci.* 1991, **84**, 13
33 Annable, T., Buscall, R., Ettelaie, R. and Whittlestone, D. *J. Rheol. (NY)* 1993, **37**, 695
34 Annable, T., Buscall, R., Ettelaie, R., Shepherd, P. and Whittlestone, D. *Langmuir* 1994, **10**, 1060
35 Gao, Z and Kwak, J. C. T. in 'Surfactants in Solution' (Eds K. L. Mittal and D. O. Shah), Vol. 11, Plenum Press, New York, 1991, pp. 261–275
36 Gao, Z., Wasylishen, R. E. and Kwak, J. C. T. *J. Phys. Chem.* 1991, **95**, 462
37 Carale, T. R. and Blankschtein, D. *J. Phys. Chem.* 1992, **96**, 459
38 Prime, K. L. and Whitesides, G. M. *J. Am. Chem. Soc.* 1993, **115**, 10714
39 Carale, T. R., Pham, Q. T. and Blankschtein, D. *Langmuir* 1994, **10**, 109
40 Cabane, B. and Duplessix, R. *J. Phys. (Paris)* 1987, **48**, 651
41 Hayakawa, K. and Kwak, J. C. T. in 'Cationic Surfactants: Physical Chemistry' (Eds D. N. Rubingh and P. M. Holland), Dekker, New York, 1991, pp. 189–248
42 Binana-Limbele, W., Clouet, F. and François, J. *Colloid Polym. Sci.* in press
43 Magny, B. Iliopoulos, I., Aubert, R., Piculell, L. and Lindman, B. *Prog. Colloid Polym. Sci.* 1992, **89**, 118